Vibrational Overtone Spectroscopy of Three-Membered Rings

Shizuka Hsieh*

Chemistry Department, Smith College, Clark Science Center, Northampton, Massachusetts 01063

Benjamin J. Miller, A. Helena Södergren, and Henrik G. Kjaergaard*

Department of Chemistry, University of Otago, P.O. Box 56, Dunedin 9054, New Zealand

Received: January 25, 2007; In Final Form: April 16, 2007

We have recorded vapor-phase photoacoustic spectra of cyclopropane, ethylene oxide, and ethylene sulfide in the third, fourth, and fifth CH-stretching overtone regions. We have used a harmonically coupled anharmonic oscillator local mode model to facilitate analysis of the spectra. Fermi resonance between the CH-stretching and HCH-bending vibrations is essential to explain the observed wide and multistructured CH-stretching overtone bands. A number of weak combination bands can account for the remaining experimental features observed to the blue of the CH-stretching regions. We have reassigned the fundamental spectra of these three-membered rings.

Introduction

Cyclopropane (C_3H_6), ethylene oxide (C_2H_4O), and ethylene sulfide (C_2H_4S) are some of the smallest existing ring systems. These three-membered rings have been of interest to chemists because of their strained geometry and unique bonding. Their small size and the availability of infrared and Raman experimental data also made them suitable for early computational predictions of vibrational frequencies and intensities.[1−10] Allen et al. accompanied their own experimental vibrational spectra of ethylene sulfide with a summary of previous experimental work and with ab initio harmonic frequencies at the SCF/6-31G* level.[1] Simandiras et al.[2] and Komornicki et al.[4] calculated vibrational frequencies and intensities at the MP2/DZP and SCF/6-31G** levels for both cyclopropane and ethylene oxide. They, along with Dutler and Rauk,[11] used their calculations for ethylene oxide to refine the interpretation of the experimental infrared spectra by Nakanaga.[5,6] The computational studies from the 1980s provide useful summaries of experimental frequencies, as do more recent reviews for ethylene oxide[12] and ethylene sulfide.[13]

While these small three-membered ring molecules provide good cases for testing theory, investigations of their CH-stretching overtone spectra have been limited to cyclopropane and monosubstituted cyclopropanes. The CH-stretching overtone spectra have been reported for cyclopropane in the regions corresponding to $\Delta v_{CH} = 3$ and $5-8$.[14−17] Wong et al. found the CH-stretching local mode frequency in cyclopropane to be very high, with a frequency about 150 cm^{-1} higher than found in other cyclic alkanes such as cyclohexane.[16] Ahmed and Henry, who measured the liquid-phase CH-stretching overtone spectra in the $\Delta v_{CH} = 2-6$ regions of monosubstituted cyclopropanes, attributed the high CH-stretching frequencies to ring strain and bonding in the three-membered ring.[18] A similar high CH-stretching local mode frequency was found in the gas-phase overtone spectra recorded of cyclopropylamine in the regions corresponding to $\Delta v_{CH} = 2-7$.[19]

The harmonically coupled anharmonic oscillator (HCAO) local mode model has been shown to simulate CH-stretching transitions in overtone spectra successfully.[18−23] When combined with electronic structure calculations of the dipole moment function, relative and absolute intensities can also be predicted well.[24−27] In the present paper we apply the HCAO local mode model to describe the dominant CH-stretching transitions. We use the Fermi resonance polyad model of Dübal and Quack to test if the commonly found Fermi resonance between CH stretch and HCH bend vibrations has any effect on our spectra.[28] The weak transitions seen to the blue of the dominant CH-stretching transitions are assigned as combination bands between CH-stretching local mode transitions and lower frequency fundamental vibrations.

Experimental Section

The gas-phase samples of cyclopropane (99%) and ethylene oxide (99.5%) were used as supplied from Aldrich. The liquid-phase sample ethylene sulfide (98%) also from Aldrich was used after a freeze−pump−thaw cycle to remove dissolved gases.

Frequency-doubled light from a Nd:YAG laser (Spectra Physics LAB150, 10 ns pulses at 10 Hz) pumped a dye laser (Sirah Cobra Stretch) to generate visible light with a line width under 0.05 cm^{-1} at 600 nm. The photoacoustic cell consists of a glass cylinder of 2.5 cm diameter and 35 cm length, with removable windows mounted at Brewster's angle, gas inlet/outlet valves, and a microphone (Knowles EK-3132) positioned near the center of the cell. The pressure of cyclopropane and ethylene oxide was maintained at 275 Torr, where the photoacoustic signal was strong and robust to ±25 Torr changes in pressure. Liquid ethylene sulfide was kept on ice to provide a constant pressure of 80 Torr in the cell. The pressure was measured on a gauge attached to the cell. After a series of prisms, the laser entered the photoacoustic cell near the center with an approximate distance from the laser beam to microphone of 1.5 cm. We monitored the amplified microphone signal as a function of laser wavelength to collect photoacoustic spectra. Laser pulse energies measured at the gas cell ranged from 5 to 50 mJ, and a thermopile power meter (Ophir AP-10) at the

* Corresponding authors. E-mail: shsieh@email.smith.edu; henrik@alkali.otago.ac.nz.

10.1021/jp070636d CCC: $37.00
Published on Web 06/01/2007

TABLE 1: Experimental and Calculated Bond Lengths (Å) and Angles (deg)

	cyclopropane (X = C)		ethylene oxide (X = O)		ethylene sulfide (X = S)	
	exptl[a]	calcd[b]	exptl[c]	calcd[b]	exptl[c]	calcd[b]
R_{C-X}			1.436	1.430 (1.436)	1.819	1.832
R_{C-C}	1.510	1.505	1.472	1.464 (1.469)	1.492	1.477
R_{C-H}	1.074	1.081	1.082	1.085 (1.085)	1.078	1.082
∠C−X−C	60	60	61.4	61.6 (61.5)	48.4	47.6
∠H−C−H	115.9	114.2	116.7	115.6 (116.3)	116.0	115.0

[a] From microwave studies of cyclopropane-1,1-d_2 by Endo and Chang.[41] [b] B3LYP/aug-cc-pVTZ optimizations and the CCSD(T)/aug-cc-pVTZ results for ethylene oxide in parentheses. [c] From Cunningham, Jr., et al.[42] and for ethylene sulfide assuming that their reported C−C−S bond angle is actually the C−S−C bond angle, as would be consistent with their reported bond lengths.

output end of the cell monitored the laser power during scans. The linear dependence of the photoacoustic signal on laser power was verified, and recorded spectra were normalized for variations in laser power. The laser wavelength was calibrated by taking photoacoustic spectra of water vapor and comparing line positions against known values. This results in wavenumber accuracy better than 1 cm^{-1}. Spectra in each overtone region required use of more than one laser dye (LDS867 and LDS821 for $\Delta v_{CH} = 4$; LDS751, LDS750, and LDS 698 for $\Delta v_{CH} = 5$; and R640, R610, and R590 for $\Delta v_{CH} = 6$). Several nanometers of overlap between scans using different dyes allowed for compilation of continuous spectra.

Theory and Calculations

The structures of cyclopropane, ethylene oxide, and ethylene sulfide have either six (for cyclopropane) or four (for ethylene oxide and ethylene sulfide) equivalent CH bonds arranged in either three or two methylene CH_2 groups. In the zeroth order approximation these CH oscillators can be modeled as isolated anharmonic local mode oscillators.[21] The coupling between CH-stretching oscillators is usually only significant if the oscillators share a common heavy atom, and we have limited the coupling to this case.[25] We have calculated peak intensities and positions for the CH-stretching overtones using the harmonically coupled anharmonic oscillator (HCAO) local mode model. The Hamiltonians for two coupled CH-stretching oscillators have been given elsewhere, and we refer to these earlier papers for details.[24,26] The HCAO local mode model requires local mode parameters, an effective coupling parameter, and a dipole moment function. The local mode oscillators are described by the local mode frequency and anharmonicity, $\tilde{\omega}$ and $\tilde{\omega}x$, respectively. These are obtained either from ab initio calculated force constants[27] or from a Birge−Sponer fit of the experimentally observed band maxima of the $\Delta v_{CH} = 4$, 5, and 6 transitions. The coupling between the two equivalent local modes contains both kinetic and potential energy contributions and can be described by an effective coupling parameter γ', which in turn can be estimated from ab initio calculations of the structure (G-matrix) and force constants.[24,26]

The dimensionless oscillator strength f_{eg} of a vibrational transition from the ground state g to an vibrational excited state e is given by[24]

$$f_{eg} = 4.702 \times 10^{-7}\ [\text{cm D}^{-2}]\ \tilde{\nu}_{eg}|\vec{\mu}_{eg}|^2 \qquad (1)$$

where $\tilde{\nu}_{eg}$ is the transition frequency in cm^{-1} and $\vec{\mu}_{eg} = \langle e|\vec{\mu}|g\rangle$ is the transition dipole moment in debye (D). The dipole moment function needed in eq 1 is approximated by a Taylor series expansion in the internal CH displacement coordinates about the equilibrium geometry, as described elsewhere.[24,26] The coefficients in the dipole expansion are obtained from a two-dimensional dipole moment grid that is calculated by displacing the hydrogen atoms of the CH bonds by ±0.2 Å from the equilibrium position in steps of 0.05 Å along the axis of the bond. The energies from these grids also provide the force constant required in the calculation of γ'.[24] It has been found previously that nine-point grids are adequate to describe the potential force constants and the dipole moment expansion coefficients.[29] We use the second, third, and fourth order force constants, from the diagonal grids, to calculate the local mode parameters.[27]

We have used density functional theory (DFT) with the B3LYP correlation functional combined with the aug-cc-pVTZ basis set. The dipole moments were calculated as analytical derivatives of the energy, and a "tight" convergence criterion was used in the geometry optimizations (gradient = 1×10^{-5} au, step size = 1×10^{-5} au, energy = 1×10^{-7} au). For ethylene oxide, the molecule that has the smallest number of basis functions in the ab initio calculation, we also optimized the structure and calculated a one-dimensional (1D) CH-stretching grid with the coupled cluster with single and double excitations including perturbative triples [CCSD(T)] levels of theory combined with the aug-cc-pVTZ basis sets. From this 1D grid we determined force constants and hence the CH-stretching local mode parameters $\tilde{\omega}$ and $\tilde{\omega}x$.[27] These calculations were done with MOLPRO 2002.6.[30] To facilitate analysis of the previous fundamental spectra and assignment of combination bands, we calculated harmonic frequencies of the vibrational normal modes with the B3LYP/aug-cc-pVTZ method. These calculations were done with Gaussian03.[31] In addition we optimized ("tight") the structures with the CCSD/aug-cc-pVDZ method using Gaussian03 and performed a natural bond orbital (NBO) analysis.[31,32]

Results and Discussion

The calculated and experimental geometric parameters of the three-membered rings are compared in Table 1. The B3LYP/aug-cc-pVTZ calculated parameters are in reasonable agreement with the experimental values. The B3LYP/aug-cc-pVTZ optimized geometries in Z-matrix form are given in the Supporting Information. For the smallest of the molecules (in computational sense), ethylene oxide, we also optimized the structure with the CCSD(T)/aug-cc-pVTZ method, which is given in parentheses in Table 1. The CCSD(T)/aug-cc-pVTZ geometry is in excellent agreement with the experimental structure and slightly better than the B3LYP/aug-cc-pVTZ method. In addition we optimized the structures with the CCSD/aug-cc-pVDZ method (not shown) and for ethylene sulfide also CCSD combined with the aug-cc-pV(D+d)Z basis set, a basis set specifically designed for second row elements such as sulfur.[33] This basis set improved R_{C-S} but had little effect on the other parameters. The B3LYP structures were slightly better than the CCSD structures.

TABLE 2: Vibrational Frequencies (in cm^{-1}) for Cyclopropane

mode	description	calcd[a]	obsd[b]
ν_1 (A_1')	CH stretch	3134	3027[c]
ν_2 (A_1')	CH_2 scissor + CC stretch	1519	1479
ν_3 (A_1')	CC stretch	1211	1188
ν_4 (A_2')	CH_2 wag	1095	1070
ν_5 (A_1'')	CH_2 twist	1153	1126
ν_6 (A_2'')	CH stretch	3220	3102
ν_7 (A_2'')	CH_2 rock	861	854
ν_8 (E')	CH stretch	3127	3024
ν_9 (E')	CH_2 scissor	1476	1439[d]
ν_{10} (E')	CH_2 wag	1052	1028
ν_{11} (E')	CC stretch	879	868
ν_{12} (E'')	CH stretch	3199	3082
ν_{13} (E'')	CH_2 rock + CC plane	1213	1188
ν_{14} (E'')	CH_2 twist	742	739

[a] B3LYP/aug-cc-pVTZ calculated harmonic frequencies. [b] From Duncan,[7] Levin and Pearce,[8] and Butcher and Jones[43] unless noted otherwise. [c] From Pliva et al.[9] [d] From Pliva and Johns.[44]

TABLE 3: Vibrational Frequencies (in cm^{-1}) for Ethylene Oxide

mode	description	calcd[a]	obsd[b]
ν_1 (A_1)	CH stretch	3093	3024
ν_2 (A_1)	CH_2 scissor	1538	1498
ν_3 (A_1)	CC/CO stretch	1299	1270
ν_4 (A_1)	CH_2 wag	1149	1159[c]
ν_5 (A_1)	CC/CO stretch	888	877
ν_6 (A_2)	CH stretch	3166	3065
ν_7 (A_2)	CH_2 rock	1177	1150[d]
ν_8 (A_2)	CH_2 twist	1048	1020
ν_9 (B_1)	CH stretch	3180	3065
ν_{10} (B_1)	CH_2 twist	1169	1147
ν_{11} (B_1)	CH_2 rock	820	808
ν_{12} (B_2)	CH stretch	3087	2978
ν_{13} (B_2)	CH_2 scissor	1505	1470
ν_{14} (B_2)	CH_2 wag	1168	1120[c]
ν_{15} (B_2)	CO stretch	843	822

[a] B3LYP/aug-cc-pVTZ calculated harmonic frequencies. [b] Experimental values taken from Nakanaga unless specified.[5,6] [c] Values reversed as suggested by Simandiras et al.[2] [d] From neutron inelastic scattering from the solid at 5 K.[45]

TABLE 4: Vibrational Frequencies (in cm^{-1}) for Ethylene Sulfide

mode	description	calcd[a]	obsd[b]
ν_1 (A_1)	CH stretch	3125	3014
ν_2 (A_1)	CH_2 scissor	1497	1457
ν_3 (A_1)	CC/CS stretch	1141	1110
ν_4 (A_1)	CH_2 wag	1045	1024
ν_5 (A_1)	CC/CS stretch	621	627
ν_6 (A_2)	CH stretch	3201	3088
ν_7 (A_2)	CH_2 rock	1200	1175
ν_8 (A_2)	CH_2 twist	899	895
ν_9 (B_1)	CH stretch	3215	3088
ν_{10} (B_1)	CH_2 twist	954	945
ν_{11} (B_1)	CH_2 rock	837	824
ν_{12} (B_2)	CH stretch	3124	3013
ν_{13} (B_2)	CH_2 scissor	1475	1436
ν_{14} (B_2)	CH_2 wag	1079	1051
ν_{15} (B_2)	CS stretch	660	660

[a] B3LYP/aug-cc-pVTZ calculated harmonic frequencies. [b] Taken from a review by Dorofeeva and Gurvich.[13]

Tables 2−4 summarize the observed fundamental vibrational frequencies available in the literature and compare them against our B3LYP/aug-cc-pVTZ calculated harmonic frequencies for the three-membered rings. B3LYP calculated harmonic frequencies are often used for comparison with observed fundamental transitions since the error in the B3LYP force field is approximately balanced by the lack of anharmonicity in the harmonic frequencies. Our assignment of the vibrational modes and their description are based on the previous observations and our B3LYP calculated vibrational normal modes and for some modes differ from the literature assignment. The agreement between the B3LYP/aug-cc-pVTZ calculated harmonic frequencies and observed fundamental frequencies is well within ~40 cm^{-1}, apart from the CH-stretching modes. The larger discrepancy (~100 cm^{-1}) for the CH-stretching modes is not surprising considering their large anharmonicities.

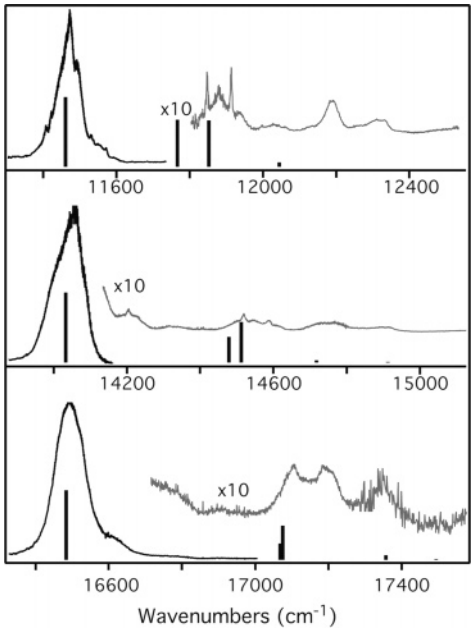

Figure 1. Room-temperature vapor-phase overtone spectra of cyclopropane in the $\Delta v_{CH} = 4$ (top), $\Delta v_{CH} = 5$ (middle), and $\Delta v_{CH} = 6$ (bottom) regions. The HCAO calculated CH-stretching transitions are indicated with sticks. The stick height corresponds to the relative oscillator strength for each transition. Both spectra and calculated transitions are expanded vertically in the regions to the blue of the main band.

Our measured gas-phase photoacoustic spectra in the $\Delta v_{CH} = 4-6$ regions of the three-membered rings are shown in Figures 1 −3. Our spectra of cyclopropane in the $\Delta v_{CH} = 5$ and 6 regions are similar to those previously published.[16,17] In Figures 1−3, the weak bands to the blue of the main CH-stretching band have been enhanced. For all three molecules the overtone spectra are dominated by the region around the pure local mode CH-stretching overtones, $|v,0\rangle_{\pm}$, as expected.

Bands in our photoacoustic spectra show some rotational structure for transitions with $\Delta v_{CH} < 6$. The loss of structure at higher quanta is consistent with homogeneous broadening due to increased IVR rates at higher energies and higher densities of states.[17,34] None of the molecules are expected to have any overtone-induced reactions that would decrease the lifetimes of the vibrationally excited states. While earlier calculations indicate that the barrier for ethylene oxide isomerization to acetaldehyde (46 kcal/mol) would be energetically accessible in the $\Delta v_{CH} = 6$ region,[35] more recent work indicates the barrier to be too high (59 kcal/mol) for isomerization at $\Delta v_{CH} = 6$.[36]

To emphasize the band shapes further, Figure 4 focuses on the main CH-stretching band in the $\Delta v_{CH} = 5$ region for all three molecules. For each, a local mode model would predict basically a single band in the overtone spectra, since all the CH bonds are equivalent.[21] The overtone spectra of benzene is one example.[23,37] In contrast, however, the three-membered rings show multistructured bands not only in the $\Delta v_{CH} = 5$ region

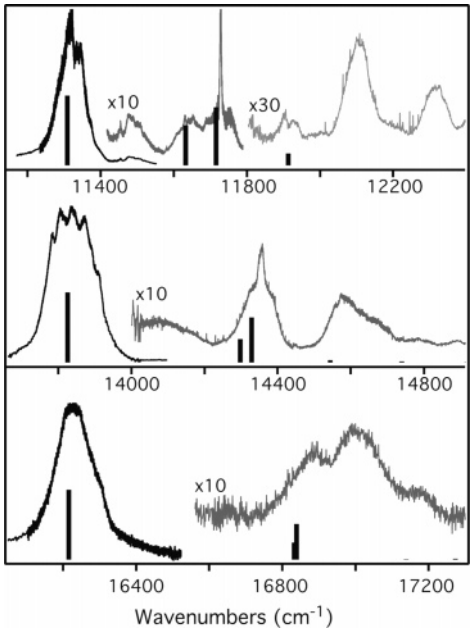

Figure 2. Room-temperature vapor-phase overtone spectra of ethylene oxide in the $\Delta v_{CH} = 4$ (top), $\Delta v_{CH} = 5$ (middle), and $\Delta v_{CH} = 6$ (bottom) regions. The HCAO calculated CH-stretching transitions are indicated with sticks. The stick height corresponds to the relative oscillator strength for each transition. Both spectra and calculated transitions are expanded vertically in the regions to the blue of the main band.

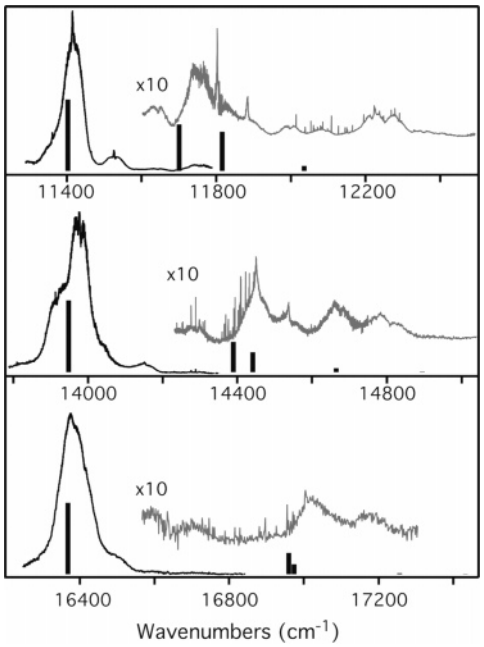

Figure 3. Room-temperature vapor-phase overtone spectra of ethylene sulfide in the $\Delta v_{CH} = 4$ (top), $\Delta v_{CH} = 5$ (middle), and $\Delta v_{CH} = 6$ (bottom) regions. The HCAO calculated CH-stretching transitions are indicated with sticks. The stick height corresponds to the relative oscillator strength for each transition. Both spectra and calculated transitions are expanded vertically in the regions to the blue of the main band.

but also in the $\Delta v_{CH} = 4$ and 6 regions although to a lesser extent. As discussed in more detail below, we attribute this complexity to Fermi resonance between the CH-stretching and HCH-bending modes. The significant widening of the $\Delta v_{CH} = 5$ band in the ethylene oxide compared to the $\Delta v_{CH} = 4$ and 6 bands (Figure 2) could suggest an additional resonance with other modes for the $\Delta v_{CH} = 5$ band.

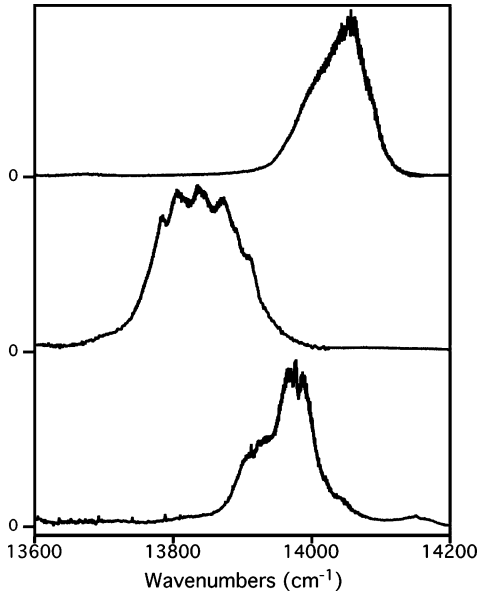

Figure 4. Room-temperature vapor-phase CH-stretching overtone spectra of cyclopropane (top), ethylene oxide (middle), and ethylene sulfide (bottom) in the $\Delta v_{CH} = 5$ region.

TABLE 5: Local Mode Parameters (cm^{-1})

	$\tilde{\omega}$		$\tilde{\omega}x$	
	calcd[a]	exptl	calcd[a]	exptl
cyclopropane	3168.3	3169	55.6	59.9
ethylene oxide	3134.7 (3162.0)	3146	60.5 (59.3)	63.0
ethylene sulfide	3167.9	3166	61.6	62.2

[a] With the B3LYP/aug-cc-pVTZ method and for ethylene oxide with the CCSD(T)/aug-cc-pVTZ method shown in parentheses.

Local Mode Parameters. Frequencies of the observed pure local mode transitions are required to determine experimental local mode parameters. Clearly this is difficult when the bands are wide like that for the $\Delta v_{CH} = 5$ region of ethylene oxide. We have used band maxima or, if visible, Q-branch-like features to estimate the pure local mode peak positions (listed in Supporting Information Table S1). The resulting frequencies carry more uncertainty than those for molecules whose CH-stretching transitions appear as single peaks. For the three-membered rings, therefore, the transition frequencies chosen for each overtone introduce uncertainty in addition to that from the standard deviation of the straight line Birge−Sponer fit. Furthermore, Fermi resonance can shift the most intense portion of the band away from the expected position for a single CH-stretching peak.[38] For these reasons we have not included uncertainties on experimental $\tilde{\omega}$ and $\tilde{\omega}x$ values in Table 5, but estimate these to be less than 20 cm^{-1} and 2 cm^{-1} for $\tilde{\omega}$ and $\tilde{\omega}x$, respectively. Observation of additional transitions and/or spectra of selectively deuterated molecules, which are unlikely to be complicated to the same extent by Fermi resonance, would reduce this uncertainty. For cyclopropane, the molecule for which the overtone bands have the least amount of structure, the frequency determination is reasonable, and our experimental local mode parameters are in good agreement with the values found previously of $\tilde{\omega} = 3175 \pm 4$ cm^{-1} and $\tilde{\omega}x = 60.4 \pm 0.6$ cm^{-1} obtained from fitting of additional ($\Delta v_{CH} = 1, 3, 5-8$) transitions.[16] These values also compare favorably with the experimental parameters obtained from fitting of the $\Delta v_{CH} = 2-7$ transitions for the two nonequivalent methylene CH-stretching local modes in cyclopropylamine, $\tilde{\omega} = 3160 \pm 4$

(3174 ± 5) cm^{-1} and $\tilde{\omega}x = 58.6 \pm 0.6$ (59.3 ± 0.9) cm^{-1}, respectively.[19]

In addition we have calculated the local mode parameters with the B3LYP/aug-cc-pVTZ method and list these in Table 5. Our calculated frequencies and anharmonicities are within 11 cm^{-1} and 5 cm^{-1}, respectively, of our experimental values and have the same relative ordering as the experimental values. Since the agreement between the B3LYP/aug-cc-pVTZ and experimental frequency is poorest for ethylene oxide, we have also calculated its $\tilde{\omega}$ and $\tilde{\omega}x$ with the significantly better CCSD(T)/aug-cc-pVTZ method. Recently, such CCSD(T) calculations were found to provide accurate OH-stretching local mode parameters for ethylene glycol.[27] This level of theory gives a frequency that is 16 cm^{-1} higher and an anharmonicity that is 4 cm^{-1} lower than the experimental values. Assuming that the CCSD(T) calculations are as accurate as they were for ethylene glycol, we suspect that for ethylene oxide our experimental frequency is too low and the anharmonicity is too high. However, we have used the experimental local mode parameters in our local mode calculations.

The relative local mode frequencies for the three-membered rings follow the bond length frequency correlation: the shorter the CH bond, the higher the CH-stretching local mode frequency.[21] Ethylene sulfide and cyclopropane have higher CH-stretching frequencies and shorter CH bonds compared to ethylene oxide. It is also interesting to note that the relative local mode frequencies of the three molecules are ordered similarly to the electronegativities of the O, S, and CH_2 fragments. Oxygen is substantially more electronegative compared to S and CH_2 which have similar electronegativities. Ahmed and Henry attribute the high CH-stretch frequency for cyclopropane rings to the unusually high p-character in the ring's strained CC bonds, which in turn causes increased s-character in the CH bonds.[18] NBO calculations show that the extent of C s-character in the CH bonds is highest for ethylene oxide, and thus, based on the extent of s-character alone, one would expect ethylene oxide to have the highest frequency, not the lowest. Thus the increased s-character is not likely to be the full explanation. Donation of lone pairs into the CH antibonding orbital weakens the CH bond and leads to a longer and weaker bond in both ethylene oxide and sulfide. Second-order perturbation theory estimates within the NBO basis show this lone pair donation to be larger in ethylene oxide than in ethylene sulfide. Thus, a combination of lone pair donation and s-character could qualitatively account for the relatively weak bond in ethylene oxide and the similarity between ethylene sulfide and cyclopropane frequencies in the series of three-membered rings. Other effects might also contribute, but it is likely that no single effect determines the relative frequencies in this series of three-membered rings.

The B3LYP/aug-cc-pVTZ calculated effective coupling parameters γ' for the three-membered ring molecules are in the range of 37−40 cm^{-1}, which is similar to the 40 cm^{-1} calculated for cyclopropylamine or the 33 cm^{-1} deduced from observed transitions.[19] All of these are significantly higher than the approximately 15 cm^{-1} coupling found for cyclohexane.[26] This large difference arises in part from the relatively large HCH angle of 116° in the three-membered rings, compared to cyclohexane's 106°, which causes a larger kinetic energy coupling in the three-membered rings.[19]

Local Mode Calculations. The HCAO calculated frequencies and intensities of the CH-stretching transitions in the three-membered rings are given in the Supporting Information Tables S2−S4. We have calculated these with the experimental local mode parameters of Table 5 and the B3LYP/aug-cc-pVTZ dipole moment function. To compare the HCAO calculated peak positions and intensities with our photoacoustic spectra, we present the HCAO results as sticks in Figures 1−3. The energy separation between the two pure local mode transitions, $|v,0\rangle_+$ and $|v,0\rangle_-$, decreases with increasing v so that they are nearly degenerate for $\Delta v_{CH} \geq 4$. The sticks in the main band therefore represent the combined calculated oscillator strength from these two transitions. The HCAO local mode model also predicts transitions to weaker local mode combination states, for example $|v-1,1\rangle_+$ and $|v-1,1\rangle_-$ transitions corresponding to one quantum in one CH-stretching oscillator and the remaining $v - 1$ quanta in the other. These transitions occur to the blue of the pure local mode transitions and have approximately one-tenth the intensity of the pure local mode transitions. The experimental spectra shown in Figures 1−3 all have features to the blue of the main band that are consistent in relative intensities with the HCAO predictions. Thus it is clear from the Figures 1−3 that the simple HCAO local mode calculation accounts for the dominant features of the overtone spectra.

TABLE 6: Calculated Total CH-Stretching Intensities[a]

v	cyclopropane	ethylene oxide	ethylene sulfide
1	2.0×10^{-5}	1.6×10^{-5}	7.2×10^{-6}
2	4.7×10^{-7}	3.9×10^{-7}	6.2×10^{-7}
3	5.4×10^{-8}	4.8×10^{-8}	5.1×10^{-8}
4	4.1×10^{-9}	4.1×10^{-9}	3.9×10^{-9}
5	3.8×10^{-10}	4.0×10^{-10}	3.5×10^{-10}
6	4.8×10^{-11}	4.9×10^{-11}	4.9×10^{-11}

[a] From HCAO local mode calculation with experimental local mode parameters and B3LYP/aug-cc-pVTZ calculated γ' values and dipole moment functions. The intensities for cyclopropane are for three CH_2 groups and for ethylene oxide and ethylene sulfide for two CH_2 groups.

The total CH-stretching intensities for pure local mode and local mode combination transitions for the various overtones are given in Table 6. The calculated total intensities for all three molecules show an approximately 10-fold drop in intensity with each quantum increase in CH stretch, which is consistent with expectation.[39] It is interesting that the fundamental transition intensity for ethylene sulfide is significantly weaker than for the other two molecules, whereas for the overtones all three molecules have similar intensity. This illustrates again that overtone intensities cannot be predicted based on fundamental intensities.[40] As cyclopropane has six CH bonds versus four in each of the other two molecules, one would perhaps have expected higher intensities for cyclopropane. Table 6 illustrates that the number of CH oscillators cannot be used as a simple indicator of relative overtone intensities in the case of heteroatom rings.[15,26]

We do not obtain absolute intensities in our photoacoustic spectra. However, Wong and Moore have measured the absolute intensities of the main band in the $\Delta v_{CH} = 5$ and 6 regions for cyclopropane[16] and obtain oscillator strengths of 4.6×10^{-10} and 6.9×10^{-11}, respectively.[15,26] Our calculated combined intensity of the $|v,0\rangle_+$ and $|v,0\rangle_-$ transitions, which comprise the main band, is 3.4×10^{-10} and 4.5×10^{-11}, respectively, in reasonable agreement with experimental values.

In Table 7 we show the total CH-stretching fundamental intensity calculated with the HCAO local mode model and with a harmonic normal mode approach (harmonic normal modes and linear dipole moment function expansion) as found in most electronic structure programs. The differences between HCAO and harmonic intensities indicate that anharmonic wavefunctions and nonlinear dipoles can make a significant difference to fundamental intensity calculations.

TABLE 7: HCAO and Harmonic Fundamental Intensities[a]

method	cyclopropane	ethylene oxide	ethylene sulfide
harmonic	1.5×10^{-5}	1.8×10^{-5}	5.8×10^{-6}
HCAO	2.0×10^{-5}	1.6×10^{-5}	7.2×10^{-6}

[a] Calculated with the B3LYP/aug-cc-pVTZ level method. Harmonic intensities are obtained with harmonic normal modes and linear dipole approximations. HCAO calculations as described in Table 6.

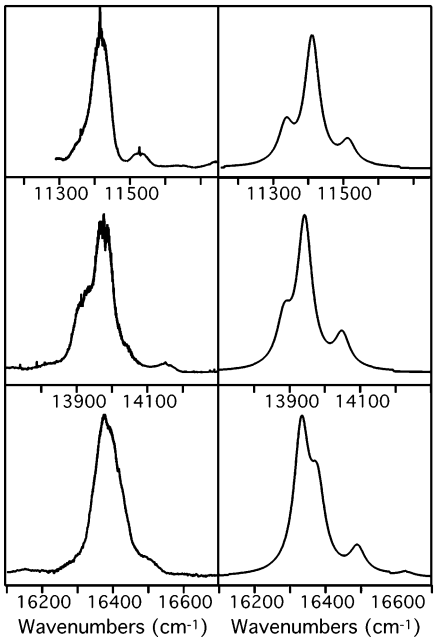

Figure 5. Experimental (left) and simulated (right) main bands for ethylene sulfide in the $\Delta v_{CH} = 4$ (top), $\Delta v_{CH} = 5$ (middle), and $\Delta v_{CH} = 6$ (bottom) regions. Peak positions and intensities for the simulations are from the Fermi resonance model of Dübal and Quack with the following arbitrary parameters: $\tilde{\nu}_s = 3100$ cm^{-1}, $\tilde{\nu}_b = 1450$ cm^{-1}, $x_{ss} = -62$ cm^{-1}, $x_{sb} = -29$ cm^{-1}, $x_{bb} = -10$ cm^{-1}, and $k_{sbb} = 35$ cm^{-1}. Each transition has been convoluted with Lorenztians with full-widths at half-maximum of 50 cm^{-1} to represent homogeneous line broadening.

Fermi Resonance. The structure within each of the main bands as well as minor peaks in the close vicinity of the main band are likely due to Fermi resonance between the dominant pure local mode CH-stretching transition and lower frequency HCH-bending vibrations. These bending vibrations (CH_2 scissor, in Tables 2−4) have frequencies that are approximately half that of the CH-stretching vibrations and ideal for Fermi resonance interactions. Simulation to illustrate the effects of Fermi resonances between the CH stretch and HCH bend was done with the polyad model of Dübal and Quack.[28] Briefly, this 2D model includes one stretching and one bending vibration and couplings between these modes, including off-diagonal terms to describe the Fermi resonance. The model assumes that the pure CH-stretching mode is the bright state, and it assigns relative intensities within a given overtone region (polyad) according to the calculated extent of bright-state character in each peak. Reasonable parameters lead to plausible simulations of the main bands. To illustrate this we show simulations for ethylene sulfide in Figure 5. The simulated spectra were obtained by convoluting each Fermi resonance transition with a 50 cm^{-1} wide Lorentzian. The good agreement between simple one stretch and one bend Fermi resonance simulations and the experimental data support our interpretation that most of the structure of the main band is due to Fermi resonance.

Local−Normal Combination Peaks. Peaks that are attributable neither to Fermi resonance nor to local mode peaks are most likely local mode−normal mode combination bands. Within a given overtone region such peaks generally appear to the blue of the pure local mode transitions. While some of these peaks could also be attributed to local mode combination transitions (Figures 1−3), we have explored tentative assignments for these weak peaks as local−normal combinations and list these in the Supporting Information Table S5.

For all three overtone regions, cyclopropane has a set of peaks ~730 cm^{-1} and ~870 cm^{-1} to the blue of each main CH-stretching band (Figure 1). We attribute the first set to combinations involving the lowest frequency CH_2 twist mode and the second set to combinations involving either the low-frequency CC stretch or CH_2 rock, (Table 2). Similarly, ethylene oxide has sets of peaks ~800 cm^{-1} and ~1000 cm^{-1} to the blue of each main CH-stretching band (Figure 2), likely involving combinations with the CH_2 rock and CH_2 twist, respectively (Table 3). Ethylene sulfide, with its many low-frequency vibrational modes, does not show as clear a pattern of peak sets, yet peaks attributable to combinations involving CC/CS stretch, CS stretch, CH_2 rock, and CH_2 twist do appear (Table S5).

Conclusion

We have recorded vapor-phase photoacoustic spectra of cyclopropane, ethylene oxide, and ethylene sulfide in the CH-stretching regions corresponding to $\Delta v_{CH} = 4-6$. The cyclopropane spectra agree with previous spectra in the $\Delta v_{CH} = 5$ and 6 regions. In the spectra of ethylene oxide and ethylene sulfide significant structure is observed in the CH-stretching band, despite the equivalence of all CH bonds in each of the molecules. We can account for this structure as Fermi resonance coupling between the CH-stretching and HCH-bending vibrations. Combinations of local modes and of local and fundamental normal modes can account for the remaining weak spectral features. Analysis of the fundamental normal mode frequencies available in the literature have led to a reassignment of some of these vibrational modes. For the three-membered ring molecules we find that the CH-stretching local mode frequencies are significantly higher than for methylene groups in larger rings or alkanes.

Acknowledgment. The authors would like to thank Mac G. Brown, Anna L. Garden, Lauren Grandpre, Daryl L. Howard, Joseph R. Lane, Robert G. Linck, and Daniel P. Schofield for helpful discussions. H.G.K. is grateful to the Research Foundation at Aarhus University for a visiting professorship. This work was supported by the Research Corporation (CC5623), the Otago Research Committee (by means of the University of Otago Postgraduate Publishing Award), the Lasers and Applications Research Theme at the University of Otago, and the Marsden Fund administered by the Royal Society of New Zealand.

Supporting Information Available: Table of the Z-matrices. Table of observed and calculated band maxima. Three tables of calculated HCAO local mode frequencies and intensities. Table with local mode−normal mode combination transitions. This material is available free of charge via the Internet at http://pubs.acs.org.

References and Notes

(1) Allen, W. D.; Bertie, J. E.; Falk, M. V.; Hess, B. A., Jr.; Mast, G. B.; Othen, D. A.; Schaad, L. J.; Schaefer, H. F., III. *J. Chem. Phys.* **1986**, *84*, 4211.

(2) Simandiras, E. D.; Amos, R. D.; Handy, N. C.; Lee, T. J.; Rice, J. E.; Remington, R. B.; Schaefer, H. F., III. *J. Am. Chem. Soc.* **1988**, *110*, 1388.
(3) Spiekermann, M.; Bougeard, D.; Schrader, B. *J. Comput. Chem.* **1982**, *3*, 354.
(4) Komornicki, A.; Pauzat, F.; Ellinger, Y. *J. Phys. Chem.* **1983**, *87*, 3847.
(5) Nakanaga, T. *J. Chem. Phys.* **1980**, *73*, 5451.
(6) Nakanaga, T. *J. Chem. Phys.* **1981**, *74*, 5384.
(7) Duncan, J. L. *J. Mol. Spectrosc.* **1968**, *25*, 451.
(8) Levin, I. W.; Pearce, A. R. *J. Chem. Phys.* **1978**, *69*, 2196.
(9) Pliva, J.; Terkihasseine, M.; Lavorel, B.; Saintloup, R.; Santos, J.; Schrotter, H. W.; Berger, H. *J. Mol. Spectrosc.* **1989**, *133*, 157.
(10) Gussoni, M.; Castiglioni, C.; Zerbi, G. *Can. J. Chem.* **1985**, *63*, 2059.
(11) Dutler, R.; Rauk, A. *J. Am. Chem. Soc.* **1989**, *111*, 6957.
(12) Dorofeeva, O. V. *Thermochim. Acta* **1992**, *194*, 9.
(13) Dorofeeva, O. V.; Gurvich, L. V. *J. Phys. Chem. Ref. Data* **1995**, *24*, 1351.
(14) Bray, R. G. *Proc. Soc. Photo-Opt. Instrum. Eng.* **1981**, *286*, 9.
(15) Wong, J. S.; Moore, C. B. *J. Chem. Phys.* **1982**, *77*, 603.
(16) Wong, J. S.; MacPhail, R. A.; Moore, C. B.; Strauss, H. L. *J. Phys. Chem.* **1982**, *86*, 1478.
(17) Crofton, M. W.; Stevens, C. G.; Klenerman, D.; Guttow, J. H.; Zare, R. N. *J. Chem. Phys.* **1988**, *89*, 7100.
(18) Ahmed, M. K.; Henry, B. R. *J. Phys. Chem.* **1987**, *91*, 5194.
(19) Niefer, B. I.; Kjaergaard, H. G.; Henry, B. R. *J. Chem. Phys.* **1993**, *99*, 5682.
(20) Mortensen, O. S.; Henry, B. R.; Mohammadi, M. A. *J. Chem. Phys.* **1981**, *75*, 4800.
(21) Henry, B. R. *Acc. Chem. Res.* **1987**, *20*, 429.
(22) Child, M. S.; Halonen, L. *Adv. Chem. Phys.* **1984**, *57*, 1.
(23) Henry, B. R.; Kjaergaard, H. G. *Can. J. Chem.* **2002**, *80*, 1635.
(24) Kjaergaard, H. G.; Yu, H.; Schattka, B. J.; Henry, B. R.; Tarr, A. W. *J. Chem. Phys.* **1990**, *93*, 6239.
(25) Kjaergaard, H. G.; Henry, B. R.; Tarr, A. W. *J. Chem. Phys.* **1991**, *94*, 5844.
(26) Kjaergaard, H. G.; Henry, B. R. *J. Chem. Phys.* **1992**, *96*, 4841.
(27) Howard, D. L.; Jørgensen, P.; Kjaergaard, H. G. *J. Am. Chem. Soc.* **2005**, *127*, 17096.
(28) Dübal, H.-R.; Quack, M. *J. Chem. Phys.* **1984**, *81*, 3779.
(29) Low, G. R.; Kjaergaard, H. G. *J. Chem. Phys.* **1999**, *110*, 9104.
(30) Amos, R. D.; Bernhardsson, A.; Berning, A.; Celani, P.; Cooper, D. L. ; Deegan, M. J. O.; Dobbyn, A. J.; Eckert, F.; Hampel, C.; Hetzer, G.; Knowles, P. J.; Korona, T.; Lindh, R.; Lloyd, A. W.; McNicholas, S. J.; Manby, F. R.; Meyer, W.; Mura, M. E.; Nicklass, A.; Palmieri, P.; Pitzer, R.; Rauhut, G.; Schütz, M.; Schumann, U.; Stoll, H.; Stone, A. J.; Tarroni, R.; Thorsteinsson, T.; Werner, H.-J. *MOLPRO*, a package of ab initio programs designed by H.-J. Werner and P. J. Knowles; 2002.6 ed., 2003.
(31) Frisch, M. J.; Trucks, G. W.; Schlegel, H. B.; Scuseria, G. E.; Robb, M. A.; Cheeseman, J. R.; Montgomery Jr., J. A.; Vreven, T.; Kudin, K. N.; Burant, J. C.; Millam, J. M.; Iyengar, S. S.; Tomasi, J.; Barone, V.; Mennucci, B.; Cossi, M.; Scalmani, G.; Rega, N.; Petersson, G. A.; Nakatsuji, H.; Hada, M.; Ehara, M.; Toyota, K.; Fukuda, R.; Hasegawa, J.; Ishida, M.; Nakajima, T.; Honda, Y.; Kitao, O.; Nakai, H.; Klene, M.; Li, X. K., J. E.; Hratchian, H. P.; Cross, J. B.; Adamo, C.; Jaramillo, J.; Gomperts, R.; Stratmann, R. E.; Yazyev, O.; Austin, A. J.; Cammi, R.; Pomelli, C.; Ochterski, J. W.; Ayala, P. Y.; Morokuma, K.; Voth, G. A.; Salvador, P.; Dannenberg, J. J.; Zakrzewski, V. G.; Dapprich, S.; Daniels, A. D.; Strain, M. C.; Farkas, O.; Malick, D. K.; Rabuck, A. D.; Raghavachari, K.; Foresman, J. B.; Ortiz, J. V.; Cui, Q.; Baboul, A. G.; Clifford, S.; Cioslowski, J.; Stefanov, B. B.; Liu, G.; Liashenko, A.; Piskorz, P.; Komaromi, I.; Martin, R. L.; Fox, D. J.; Keith, T.; Al-Laham, M. A.; Peng, C. Y.; Nanayakkara, A.; Challacombe, M.; Gill, P. M. W.; Johnson, B.; Chen, W.; Wong, M. W.; Gonzalez, C.; Pople, J. A. *Gaussian 03*, Revision C.02, 2004.
(32) Weinhold, F. Natural Bond Orbital Methods. In *Encyclopedia of Computational Chemistry*.; Schleyer, P. v. R., Ed.; John Wiley & Sons, Chichester, U.K., 1998; Vol. 3, p 1792.
(33) Wilson, A. K.; Peterson, K. A.; Dunning, T. H. *J. Chem. Phys.* **2001**, *114*, 9244.
(34) Ishiuchi, S.; Fujii, M.; Robinson, T. W.; Miller, B. J.; Kjaergaard, H. G. *J. Phys. Chem. A* **2006**, *110*, 7345.
(35) Belbruno, J. J. *J. Phys. Org. Chem.* **1997**, *10*, 113.
(36) Joshi, A.; You, X.; Barckholtz, T. A.; Wang, H. *J. Phys. Chem. A* **2005**, *109*, 8016.
(37) Reddy, K. V.; Heller, D. F.; Berry, M. J. *J. Chem. Phys.* **1982**, *76*, 2814.
(38) Howard, D. L.; Kjaergaard, H. G. *J. Chem. Phys.* **2004**, *121*, 136.
(39) Quack, M. *Annu. Rev. Phys. Chem.* **1990**, *41*, 839.
(40) Kjaergaard, H. G.; Low, G. R.; Robinson, T. W.; Howard, D. L. *J. Phys. Chem. A* **2002**, *106*, 8955.
(41) Endo, Y.; Chang, M. C. *J. Mol. Spectrosc.* **1987**, *126*, 63.
(42) Cunningham, G. L., Jr.; Boyd, A. W.; Myers, R. J.; Gwinn, W. D.; Le Van, W. I. *J. Chem. Phys.* **1951**, *19*, 676.
(43) Butcher, R. J.; Jones, W. J. *J. Mol. Spectrosc.* **1973**, *47*, 64.
(44) Pliva, J.; Johns, J. W. C. *J. Mol. Spectrosc.* **1985**, *113*, 175.
(45) Coulombeau, C.; Jobic, H. *J. Mol. Struct.* **1988**, *176*, 213.